1 Introduction

In this section, I will give first a short introduction to ultracold atoms and secondly I will give a motivation and the condition of quantum computation.

1.1 Ultra Cold Atoms

Ultracold atoms is a dominant experimental apparatus that has an analogy to other real physical systems. Moreover, ultracold fermionic systems can realize as describe a fermionic physical system with a high powerful experimental toolbox. The atoms are isolated with ultrahigh vacuum from the external environment. The cooling process can divide to two parts, first by on resonance laser that can cool the atoms up to $\sim 10\,\mu$K in ^{40}K. The second part is evaporation in a magnetic or optical trap. One of the important tools in such system is Feshcach resonance, the ability to tune the interaction from strongly repulsive to attractive.

1.1.1 Feshbach resonance in cold atoms

One of the main tools in cold atom experimental is the ability to control the interaction between atoms using the Feshbach resonance mechanism. They allow to widely tune the scattering length of the atoms. The interaction between two atoms can describe with a scattering process. This depends on a single parameter — the scattering length that given by

$$a = -\lim_{k \ll 1/r_0} \frac{\tan(\delta_0)}{k}$$

where k is the scattered atom momentum, r_0 is the interaction range, and δ_0 is the phase shift between the incoming and the scattered wave-function. In alkali atoms (like ^{40}K), the scattering length is around the van der Waals atomic range $a \sim r_0 = 50 - 100a_0$, where a_0 is the Bohr radius. In this case, $1/k_F a \approx 0.03$ which is very small corresponding to weakly interaction gas. The scattering length can be tuned from negative to positive and make the atoms from attractive to repulsive, respectively.
The key to manipulating the scattering length stems from the coupling between different atomic states with different total magnetic moments. The relative offset energies between the different state can be tuned via an external magnetic field, due their different magnetic moment (Zeeman shift). Typically, the atoms enter the collision in the lowest energy channels, which called open channel. The second involved channel is called the closed channel and it has a higher energy.

The relative Zeeman shifts between these two channels can be used to tune the energy of the last bound state of the close channel into resonance with the close channel bound state. As a result, the scattering length diverges at resonance and is given by

$$a(B) = a_{bg}\left(1 - \frac{\Delta B}{B - B_0}\right) \tag{1}$$

where a_{bg} is the background scattering length away from resonance, ΔB is the resonance width, and B_0 is the resonance position. In ^{40}K the parameters for Feshbach resonance between the state $|F = 9/2, m_f = -9/2\rangle$

and $|F = 9/2, m_f = -7/2\rangle$ are:

$a_{bg} = 169.7\, a_0$, $B_0 = 202.14\,(1)$ G, $\Delta B = 6.70\,(3)$ G. There is more resonance between other states but for other reasons, we want to work in this specific states.

1.1.2 Optical dipole trap

When an electric field E oscillating with frequency ω, such as the light field, acts on a neutral atom it induces an electric dipole moment

$$p = \alpha E$$

where α is the complex polarizability. Because this electric dipole moment interacts with the light field, the atom has a potential energy of

$$U_{dip} = -\frac{1}{2} \langle pE \rangle \propto -\mathrm{Re}\,(\alpha)\, |E|^2$$

Therefore the potential energy is proportional to the intensity $I \propto |E|^2$ of the oscillating field. Taking into account the frequency dependence of and damping due to spontaneous emission, the full expression for the dipole potential is given by [11] :

$$U_{dip}(r) = \frac{3\pi c^2 \Gamma}{2\hbar \omega_{0,1}^3 \delta} I\,(r)$$

where $I\,(r)$ is the laser beam intensity, Γ is the natural line-width, and $\delta = \omega - \omega_{0,1}$ is the frequency detuning of the laser from the frequency of the optical transition $\omega_{0,1}$. The dipole trap can be attractive for red detuning ($\delta < 0$) or repulsive for blue detuning ($\delta > 0$). For the simple case of TEM_{00} Gaussian mode the depth of the potential is given by

$$U_{dip}(r, z) = -U_0 \left[1 - 2\,(r/\omega_0)^2 - (z/z_R)^2\right]$$

where ω_0 is the beam waist, z_r is the Rayleigh range and U_0 is the trap depth.

1.2 Quantum computation and simulation

In quantum mechanics, the dimension of the Hilbert space grows exponentially with the system size. In order to present a quantum state with n particles in classical computation we need an order of C^n bytes, where C is a constant. Therefore, the possibility of making a calculation of many-body quantum states becomes an impossible situation in classical computing.

To overcome this problem, it was first proposed by Richard Feynman [9] to use a quantum computational machine ("Quantum Computer"). A quantum computer is able to calculate not only simulation of quantum dynamics but also complex mathematical problems.

For two decades, researchers have been trying to implement quantum computation using different platforms. These platforms were able to make progress with, but all the systems were limited and they held back its further development.

Quantum computer system requirements as stated by D.DiVincenzo [?] should comply with the conditions:.

- **Quantum state.** The quantum state is the storage of the quantum information in a quantum computer, therefore it needs to be well defined. In quantum computation the state is usually two state ,$|0\rangle$and $|1\rangle$.These states define the qubit, and the qubit state is defined by

$$|\psi\rangle = \alpha\,|0\rangle + \beta\,|1\rangle$$

  where α and β are complex numbers. When the qubit is measured, with the probability of $|\alpha|^2$ it will be in a state $|0\rangle$ and with a probability of $|\beta|^2$ in a state $|1\rangle$, satisfying the relation:

$$|\alpha|^2 + |\beta|^2 = 1$$

  since the probabilities must total in sum to one.

- **Preparation of the Initial State.** The system should have the possibility to prepare the initial state of the qubit. The initial state is of little importance as we can enable operators ("quantum gates") to function upon the system, obtain every possible state and use them as an initial base for the system.

- **Quantum gates.** It should be possible to operate the system with a set of operators. The system should include the possibility of performing on several of universal unitary operations ("Quantum Gates"). A gate is able to act upon a one qubit or two qubit system. There are several types of one qubit gates including a Hadamard gate, a phase gate and $\pi/8$ gate. The two qubit gate is C-NOT. In place of a C-NOT gate we can use a $\sqrt{SWAP}$gate.
  By using Hadamard, Phase and $\sqrt{SWAP}$ gates we can obtain any unitary operation of n qubits by taking a cumulative series of these gates.

- **Ability to Measure the Result.** The ability to measure the final state of the system is required for all computation systems. Therefore, here we also should be able to measure the final state of the system (in all qubits).

- **System Scalability.** System physical resources (space, money, etc.) will not scale as X^n, where X is some system constant and n is the number of qubits. This requirement enables the system to become technically effective.

Another problem that exists in the real world is decoherence due to undesirable interactions between the quantum computer and its environment. Therefore, we need to make sure that the time scale of the system isolation T_I is smaller then the preparation time of all the operation gates T_{gate}.

$$\frac{T_{gate}}{T_I} \ll 1$$

To date, attempts were made to create different physical systems to meet these requirements, including optic [20], ion traps [6, 13], quantum dots [15], neutral atoms in optic trap [27] and superconductivity devices [2]. All of these systems suffer from inherent limitations that prevent them from constituting a perfect platform for quantum computation. For example, in an ion trap, charged ions can be heated by fluctuating patch potentials in trap electrodes [28].

We have developed a new platform of quantum computation which is bases upon ultracold fermi atoms in an optical microtrap. The basis for these platforms is the fact that the system has a fermionic statistic. In addition, the system of cold atoms can control the interaction between atoms by using Feshbach resonance. Furthermore, the depth of the micro-trap, shape and position in space can be controlled dynamically.

2 The new platform of quantum computation

This chapter describes how the five conditions for quantum computation are realized in our proposed computational scheme. The $\sqrt{\mathrm{SWAP}}$ gate was developed by Dr. Jonathan Nemirovsky.

2.1 The Qubit

Our quantum computer is based on two internal energy levels of a ^{40}K atom held in a microtrap. We choose $|\downarrow\rangle = |0, 9/2, -9/2\rangle$ and $|\uparrow\rangle = |0, 9/2, -7/2\rangle$ with notation $|n, F, m_f\rangle$, where n is the vibrational state, F is the total atomic spin, and m_f is the projection in $\hat{z}$ direction (set by external magnetic field). We can choose any two m_f states, but we want to control the interaction between the atoms by means of a Feshbach resonance [5]. The Feshbach resonance between $m_f = -9/2$ and $m_f = -7/2$ is at $B = 202.14$ G. This tunability is going to be important for the implementation of the two qubit gate.

2.2 Preparation Initial State

The requirement of preparation sequence is to generate a single atom in a microtrap with the ability to know the initial state. The system would be fast with high repeatability. The system will be described in more details in experimental system chapter.

2.3 Quantum Gate

To perform a quantum computer, we need to realize a single qubit gate (**Hadamard** gate, the phase gate, $\boldsymbol{\pi/8}$ gate), and the two-qubit gate$\sqrt{\text{SWAP}}$ in our system.

- Single qubit gate:
  Any unitary transformation on a single qubit can be decomposed into a rotation in the Bloch sphere around some axis $\hat{n}$ by an angle θ multiplied by a global phase ϕ

  $$U = e^{i\phi} e^{-i\frac{\theta}{2}\cdot\hat{\sigma}_n}$$

  where $\hat{\sigma}_n$ is Pauli matrices. We can realize this unitary transformation in a cold atom system by coupling some two-level system to an external EM field [1, 16]. The experimental parameters that control the Bloch sphere rotation are the phase of the RF pulse and the detuning between its frequency and the two states energy different divided by $\hbar$.

- $\sqrt{\text{SWAP}}$ gate
  The $\sqrt{\text{SWAP}}$ is a two qubit gate that swap the states half way, namely,

  $$U_{\sqrt{swap}} = \begin{bmatrix} 1 & 0 & 0 & 0 \\ 0 & \frac{1}{2}(1+i) & \frac{1}{2}(1-i) & 0 \\ 0 & \frac{1}{2}(1-i) & \frac{1}{2}(1+i) & 0 \\ 0 & 0 & 0 & 1 \end{bmatrix}$$

  with respect to the basis $|\downarrow\downarrow\rangle$, $|\downarrow\uparrow\rangle$, $|\uparrow\downarrow\rangle$, $|\uparrow\uparrow\rangle$. In Bell state representation, the $\sqrt{\text{SWAP}}$ is change just the anti-symmetric state

  $$\left(\hat{d}_1{}^\dagger \hat{u}_2{}^\dagger - \hat{u}_1{}^\dagger \hat{d}_2{}^\dagger\right)|\psi\rangle \rightarrow i\left(\hat{d}_1{}^\dagger \hat{u}_2{}^\dagger - \hat{u}_1{}^\dagger \hat{d}_2{}^\dagger\right)|\psi\rangle$$

  whereas the other states not develop.
  To implement the two-qubit $\sqrt{\text{SWAP}}$ gate, we utilize two unique advantages of ultracold atoms.

  - Ability to control the interaction between atoms around Feshbach resonance [5].
  - Ability to shape the potential landscape using far off resonance light, controlling the atom tunneling between two traps [24].

These, together with fermionic statistics, are the basis for a new protocol for $\sqrt{\text{SWAP}}$ gate. This protocol is original but similar in some aspects to the gate first described in Ref. [12]. We consider two optical microtraps with one atom at each site, with a distance $d(t)$ between them. Using second quantization formalism and the Fermi-Hubbard model [14], the Hamiltonian is given by

$$\begin{aligned} H_{J,U} &= J \cdot \left(\hat{u}_1^\dagger \hat{u}_2 + \hat{u}_2^\dagger \hat{u}_1 + \hat{d}_1^\dagger \hat{d}_2 + \hat{d}_2^\dagger \hat{d}_1\right) + 2U \cdot \left(\hat{u}_1^\dagger \hat{u}_1 \hat{d}_1^\dagger \hat{d}_1 + \hat{u}_2^\dagger \hat{u}_2 \hat{d}_2^\dagger \hat{d}_2\right) \\ &\equiv J \cdot H_J + U \cdot H_u \end{aligned}$$

Where J is the tunneling energy, U is on site interaction energy, $\hat{u}_i$ and $\hat{u}_i^\dagger$ are annihilation and creation operators of particle i in state $|\uparrow\rangle$ and $\hat{d}_i$ and $\hat{d}_i^\dagger$ are annihilation and creation operators of particle i in state $|\downarrow\rangle$. By tuning the system parameters $U = U_1$ with Feshbach resonance and $J = J_1$ with the distance between the qubits $d(t)$ and set the gate duration T_1 the dynamics of the Hamiltonian are given by

$$\sqrt{\text{SWAP}} = \exp\left(-iT_1 H(U_1, J_1)/\hbar\right)$$

The conditions on U_1 and T_1 are (see Appendix):

$$U_1 = \pm \frac{2J\hbar\left(2n - \frac{1}{2}\right)}{\sqrt{m^2 - \left(2n - \frac{1}{2}\right)^2}} \qquad\qquad T_1 = \frac{\hbar\pi\sqrt{m^2 - \left(2n - \frac{1}{2}\right)^2}}{2J}$$

Where m is an odd integer and n is any integer. The last parameter, J_1, depends on the distance between the two qubits, i.e., $d(t)$.
We can realize the $\sqrt{\text{SWAP}}$ gate in the following stages

1. We set the tunneling to some value $J = J_1$ and close the interaction $U = 0$. We wait for $t_1 = \frac{\pi\hbar}{4J_1}$ and get the dynamic for the anti-symmetric state $|\psi_A\rangle$.

$$\left(\hat{d_1}^\dagger \hat{u_2}^\dagger - \hat{u_1}^\dagger \hat{d_2}^\dagger\right)|0\rangle \rightarrow -i\left(\hat{d_1}^\dagger \hat{u_1}^\dagger + \hat{u_2}^\dagger \hat{d_2}^\dagger\right)|0\rangle$$

   while the symmetric states $\hat{d_1}^\dagger \hat{u_2}^\dagger + \hat{u_1}^\dagger \hat{d_2}^\dagger$, $\hat{u_1}^\dagger \hat{u_2}^\dagger$, $\hat{d_1}^\dagger \hat{d_2}^\dagger$ are stationary.

2. Now, we take the tunneling energy to zero, $J = 0$, and open the interaction $U = U_1$ for duration of $t_2 = \frac{\pi\hbar}{4U_1}$. As a result, the symmetric states are not change while the $|\psi_A\rangle$ state is now

$$-i\left(\hat{d_1}^\dagger \hat{u_1}^\dagger + \hat{u_2}^\dagger \hat{d_2}^\dagger\right)|0\rangle \rightarrow -\left(\hat{d_1}^\dagger \hat{u_1}^\dagger + \hat{u_2}^\dagger \hat{d_2}^\dagger\right)|0\rangle$$

3. In last stage, we repeat on the first stage by setting the tunneling energy $J = J_1$ and turn off the interaction. We wait $t_1 = \frac{\pi\hbar}{4J_1}$ and the symmetric state ,again, not change but the anti-symmetric

state $|\psi_A\rangle$ is now

$$-\left(\hat{d_1}^\dagger \hat{u_1}^\dagger + \hat{u_2}^\dagger \hat{d_2}^\dagger\right)|0\rangle \to i\left(\hat{d_1}^\dagger \hat{u_2}^\dagger - \hat{u_1}^\dagger \hat{d_2}^\dagger\right)|0\rangle$$

As we can see this is the $\sqrt{\text{SWAP}}$ gate.

2.4 Detection

After we finish encoded our atoms, we need to detect their final state. The detection of a single potassium 40 atom cant done for atoms in lattice with a fluorescence imaging on the cycling transition $|-9/2,-9/2\rangle_{^2S_{1/2}} \to |11/2,-11/2\rangle_{^2P_{3/2}}$ due to the D transition (1169 nm from the $^2P_{3/2}$) [4]. In the last years, some groups develop a new technique and I will discuss them in (4.3).

2.5 Scalability

The scalability in our scheme is fairly straightforward. The cooling sequence is the same and not require any more resources, and we can load more micro-trap and create several qubits. The position of each qubit depends on the angle beam that translates by the objective to a position in the focal plane. The distance between the trap is given by

$$\theta = f \cdot d$$

Where d is the distance between two microtraps and f is the objective focal. One way to control dynamically the relative angle θ is to use Acusto-Optic-Deflector (AOD). By placing two AOD in an orthogonal direction, we can move the position of the microtraps in the focal plane [#lester2015rapid].

3 preliminary results

On the last three years, I have been an important partner in the development of the first cold-atom system of Prof. Yoav Sagi group. In this system (which build for other requirements) we check method for the new apparatus. All the preliminary results are done on the first system that composed of three cells under ultrahigh vacuum. In the first cell (source), we release ^{40}K atoms from homemade dispensers. The atoms are captured by a 2D MOT. On the third axis, there is a mirror with a hole (nozzle) inside the chamber. The atoms are cooled in two axes and pushed to the second cell by another laser. In the second chamber (cooling), the atoms are captured by a 3D MOT. At this point, the cloud temperature is around ~ 220 μK. By using a Gray Molasses cooling on the D_1 atomic transition, the atomic cloud temperature is reduced to ~ 15 μK. Next, we optically pump the atoms into the states $|9/2,9/2\rangle$ and $|9/2,7/2\rangle$ and load them to a QUIC magnetic trap. In this configuration, we obtain a magnetic trap without zero magnetic field (this is important for RF evaporation). Following the evaporation, the temperature is $T/T_f \approx 4.5$. Next, we load the atoms into a far-off-resonance optical trap that focus to 39.5 μm with power of 6W. The optical trap is moved adiabaticly by air bearing stage to the science chamber, a distance of around 320 mm. In the science

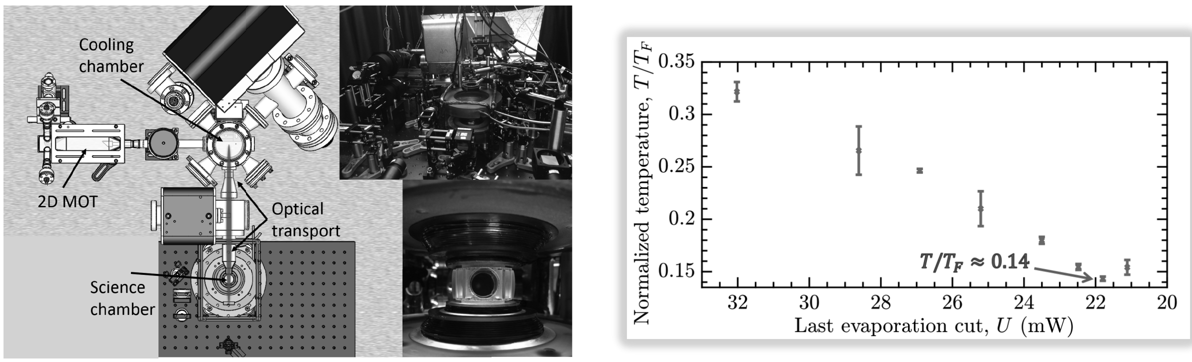

(a) (b)

Figure 1: (a) picture of the preliminary result system. (b) The final conditions of the atoms Vs. optical trap cutoff evaporation.

chamber, a second beam crossing the first one at an angle of 45° with $\omega_0 = 200\,\mu$m. Finally we get ~150,000 atoms per spin state at $T/T_F \approx 0.2$

3.1 Creating and loading a micro trap

One of the most parts of our system is the ability to create a single atom in ground state hold in optical micro-trap. In the new system we will need objective with high NA (>0.6). We build a home made objective with NA=0.3 learn how to load and detect a single atom.

3.1.1 Homemade Objective with NA=0.3

We use our simulation for ray trace and design a homemade objective from commercial lenses Table (1). As shown in (2) We simulated and found the maximum NA=0.3 with λ = 1064 nm. We design and create a holder from Ultem with a spacer from Aluminum that takes out after the lens position was fixed by glue. The objective was characterized by two independent measurements. First, we want to measured the waist ω_0 that we can get with this objective. We create a Knife edge measurement with resolution of ~50 nm (with Michelson interferometer) and get ω_0 = 2.3 μm (3). Secondly, We measured the resolution by look at the resolution target and measured the Point-Spread-Function (PSF) of μm pinhole. We used a 1951 USAF resolution target and magnification the imaging by 28 on CCD camera. The largest resolution with this target is 4.4μm. We clearly see a resolution of 4.4\mum and even more with a laser wavelength of 770 nm (the original design was for 1064 nm). We now know the imaging system magnification and can measure the PSF from the pinhole of 1.25±0.25μm. We get NA = 0.24±0.03 for PSF fitting and NA = 0.289±0.0083 for Modulation Transfer Function calculation (which is the mathematical Fourier transform of the PSF)(3).

Surface number	Catalog number	Radius [mm]	Distance to the next surface [mm]	Material
1	LC1582	∞	3.5	BK7
2	-	38.6	10.92	air
3	LB1901	76.6	4.1	BK7
4		-76.6	10	air
5	LA1608	38.6	4.1	BK7
6		∞	2	air
7	LE1234	32.1	3.6	BK7
8		82.2	21	air
9	Vacuum window	∞	3.15	Silica
10		∞	-	Vacuum

Table 1: Technical detail of the lenses. All the lenses are commercial from Thorlabs catalog.

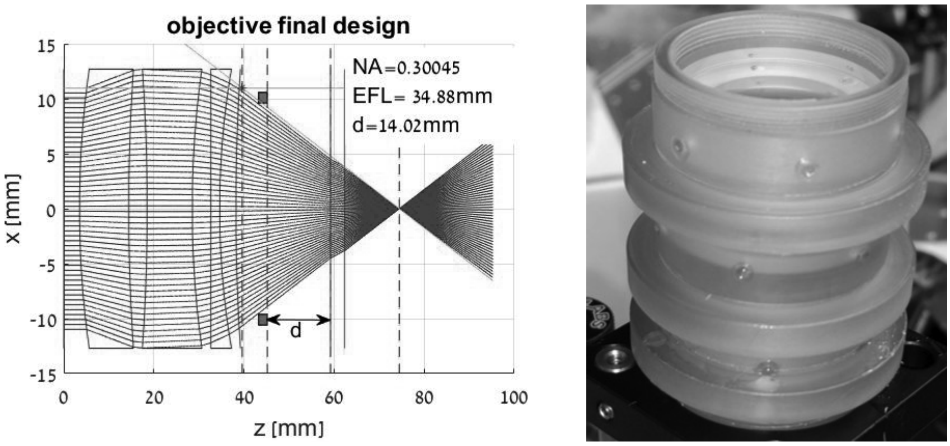

(a) (b)

Figure 2: (a) Objective ray trace simulation. (b) Picture of the objective after assembly.

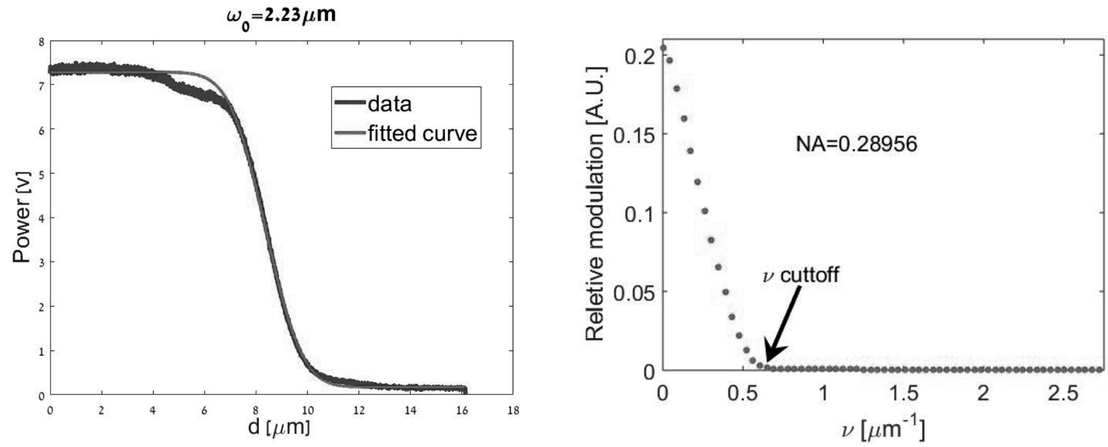

(a) (b)

Figure 3: (a) Calculation of the beam waist with knife edge technique. (b) MTF Vs frequency. The cutoff frequency is where the MTF is in order of the noise.

.

3.1.2 loading a single atom to microtrap

One of the demands of our system is the ability to create a single atom in the ground state. In degenerate Fermi gas, the occupation probability for a state with energy E is described by Fermi-Dirac statistics

$$P\left(E\right)=\frac{1}{\exp\left(\frac{E-\mu}{k_{B}T}\right)+1}$$

where μ is the chemical potential and T is the temperature. To calculate this probability, we can use $\mu\approx E_{F}=k_{B}T_{F}^{reservoare}$ and change the optical trap parameters ($T_{F}^{microtrap}$ and the ground state energy $E_{0}=\hbar\overline{\omega}$) such that

$$P\left(E_{0}\right)>0.999$$

Therefore, we stop the optical evaporation with ~300,000 atoms in $T/T_{F}\approx0.4$. Then we open the microtrap and load ~1000 atoms and turn off the optical trap. Then we lower the microtrap laser power until we get ~ 200 atoms. Then we add gradient coils that lower the total potential without change the trap frequencies. In order to load the colder atoms, the trap and the microtrap need to be at the same position. First, we used a power of ~ 200mW and insert an iris before the objective. As a result, we get high trap depth and more volume in the microtrap. As shown in figure (5), we find the microtrap position by taking absorption imaging of the atoms in the microtrap (the rest of atoms are Falling down). In these conditions, we load ~40,000

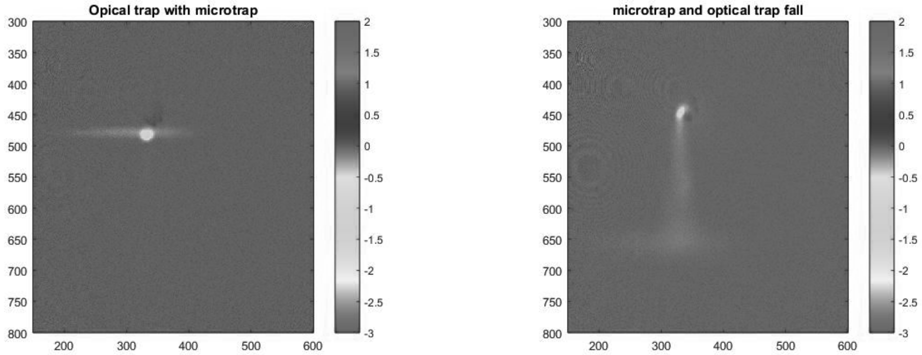

(a) (b)

Figure 5: We set the microtrap positions and take absorption imaging of the atoms cloud. In figure (a) we release the traps together and in figure (b) we give a delay of 10 msec between them. We can see that the atoms who were trapped in the microtrap are staying at the same position while the rest are following.

atoms. Then we open the iris and lower the trap depth and scan the trap position with xyz translation stage. Because the absorption signal of a single atom is low, this method cannot be used for measuring less than 4000 atoms. Therefore, the measurements were taken by 3D MOT as described in the following section. In the microtrap, the atoms lifetime is $\sim 26\,\mathrm{sec}$(4).

We build a single atom detection using 3D MOT, the MOT parameters are different from the 3D MOT in the first cooling stage. For example, in order to localize the atoms in small area, the magnetic field gradient higher and the laser frequency detuning is smaller. The photon was collected by lens ($f = 75\,mm$) with NA of 0.17 to sCMOS camera (Andor Zyla 5.5). We calculate the signal per atom in our system and is $\sim 2700\ \frac{\mathrm{count}}{\mathrm{atom\ sec}}$. Unfortunately, the background scattering photons from the chamber windows is large ($\sim 5\%$ per surface) and the ability to detected atoms are limited to ~ 5 atoms. To overcome this limit, we insert in one direction - orthogonal to imaging axis. we apply a ultra-narrow and pass filter that block the D_2 photons and the D_1 photons are transited. First, we add a laser with wavelength of the D_1 cooling and found that the signal is lower for the same number of atom with the same life time (6). But when we add a repump frequency to the

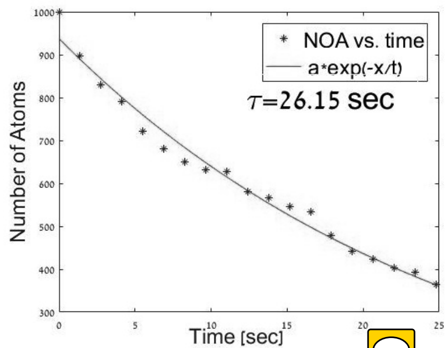

Figure 4: measurement of the atoms lifetime in the microtrap

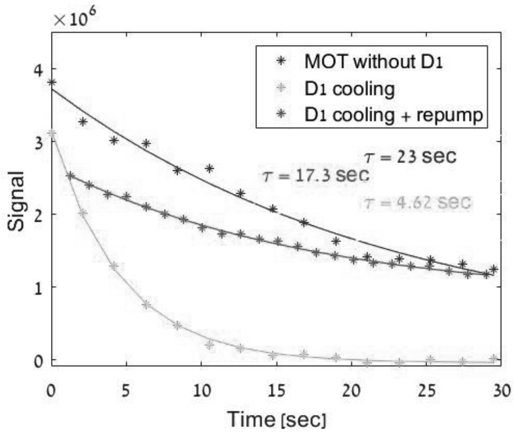

(a)

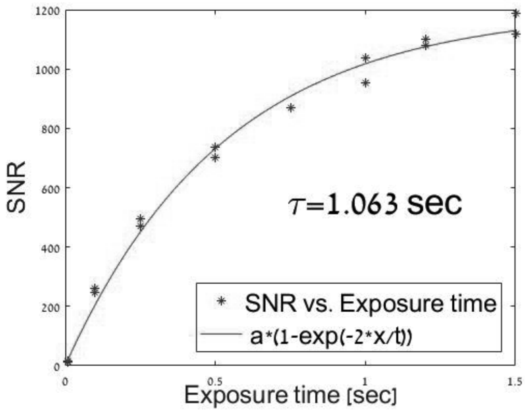

(b)

Figure 6: (a) Lifetime in 3D MOT. The 3D MOT on the D_2 is given a lifetime of 23 sec. The D_1 cooling is lower the lifetime while the D_1 repump can give the same signal and the lifetime is increase to the regular MOT lifetime. The data was taken with exposure time of 0.2 sec (b) SNR of the D_1 Vs. exposure time.

MOT beam, we get almost the same signal then the D_2 3D MOT with a long life time. These new setup are increase the SNR (for long life time) and now we can detect a single atom (6).

3.2 Sensitive RF spectroscopy [25]

The 3D MOT adds to our system a new detection ability of a small number of atoms. As a result, we can create a measurement that requires a small number of atoms detection. One of this measurement is RF spectroscopy - a measurement of the number of atoms out-coupled by the RF pulse versus its frequency. From this measurement, we can exact many physical observables. One of them is the contact C which measured the energy change due to the interaction energy between two fermions. At high frequency, contact interactions in 3D give a rise to a power-law scaling of $\Gamma(\nu)$[22].

$$\Gamma(\nu) \to \frac{C}{2^{3/2}\pi^2}\nu^{-3/2}$$

where ν is the rf frequency in unit of E_F/h and C is in unit of Nk$_F$, where N is the total number of atoms and k_F is the Fermi k-vector. The total signal is normal to $\int_{-\infty}^{\infty}\Gamma(\nu) = 1/2$. In previous work, the signal was limited to $\nu \leq 12$ E$_F$ and the signal of the contact is show up only above 5 E$_F$[26]. Using our RF spectroscopy scheme we measured up to 150-200 E$_F$ which open a new tool to calibrate the interaction parameter and directly measure the contact tail power law.

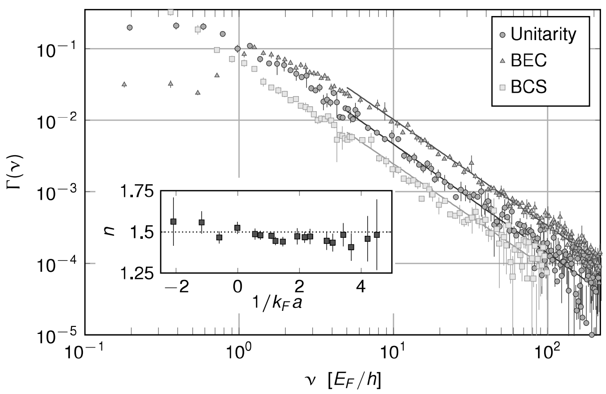

Figure 7: Lineshapes for three different interaction strengths $1/k_F a = 0$ (unitarity), $1/k_F a = 0.49$ (BEC), and $1/k_F a = -0.52$ (BCS) . Linear scaling shows that the data follows a power-law at high frequencies. The inset shows the power-law exponent extracted by fitting the tail of each dataset with c_1/ν^n.

We prepared the atoms, as described above, in balance mixture of $|1\rangle = |F = 9/2, m_f = -9/2\rangle$ and $|2\rangle = |F = 9/2, m_f = -7/2\rangle$ which have Feshbach resonance at B = 202.2 G. The magnetic field decreased to B1 = 203.4 G at 30 ms and then after more 8 ms at B1 a 400 μs RF square pulse transfer a small fraction of atoms from the $|2\rangle \to |3\rangle = |F = 9/2, m_f = -5/2\rangle$ ($\sim$ 47 MHz depend on $B1$). Still, we can't use a 3D MOT just to probe $|3\rangle$ state. Therefore, we transfer the $|3\rangle$ state with MW ramp to $|4\rangle = |F = 7/2, m_f = -3/2\rangle$. Due to their difference in the magnetic moment, the opening of magnetic gradient coils creates anti-trap for $|1\rangle$, $|2\rangle$, $|3\rangle$ states while $|4\rangle$ is trapped. Then, We wait a time that ensures that we stay just with $|4\rangle$ and open the 3DMOT. The signal of the atom is detection with Zyla 5.5 Andor camera.

We take a several line-shape with a different interaction strength and fit it with a power law function

$\Gamma(\nu) \propto \nu^{-n}$ (7). We found the results are compatible with 1.5 that show in the theoretical function.

For an attractive force, we can create a Feshbach molecule and measure the banning energy that given by

$$E_b = \frac{\hbar}{m\left(a-\bar{a}\right)^2} \qquad (2)$$

where $\bar{a}$ is the finite range correction of the van der Waals potential and a is the scattering length (1). A general form of the transition line-shape of a weakly bound molecule is given by

$$\Gamma(\nu) = \Theta\left(\nu - E_b/h\right)\frac{C}{2^{3/2}\pi^2}\frac{\sqrt{\nu - E_b/h}}{\left(\nu-\nu_\omega\right)^2} \qquad (3)$$

where Θ is Heaviside step function. We fit our data and get a deviation from the old ^{40}K parameters line that systematic increasing from the data away from the resonance, which was unmeasured yet due to the low signal. We fit our data and calibrate the Feshbach resonance parameters $B_0 = 202.15\,(1)$ G and $\Delta = 6.70\,(3)$ G using the known values and $a_{bg} = 169.7\,a_0$ [8].

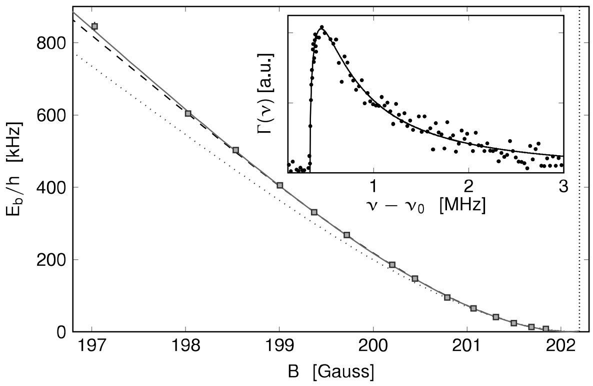

Figure 8: The binding energy of the Feshbach molecule at different magnetic fields close to the Feshbach resonance (202.2G). We extract the binding energy (squares) by fitting the rf lineshape with the molecular spectral function given by (3) (inset). The theory of equation (2) with the Feshbach resonance parameters given in Ref. [10]($B_0 = 202.20\,(2)$G, $\Delta = 7.04\,(10)$G, and $a_{bg} = 174a_0$) is a systematic divided from the experimentally data (dotted blue line). We fit our data to (2) with B_0 and Δfit parameters (dashed black line). In addition, We fit the data with a two coupled channels calculation (solid red line) based on the model of Ref. [23]

In conclusion, We have develop a new sensitive rf spectroscopy scheme in cold atoms. This is open a new experimental research that have inherent a low signal of only several atoms. We apply this method to confirm the universal behavior of a contact like potential. In addition we calibrate the Feshbach resonance parameters B_0 and Δ from the binding energy of the Feshbach molecule.

4 Research Plan

4.1 Dedicated New Experimental Apparatus

From the vast experience we have accumulated in our group over the last three years, we can accurately define the requirements of the new system.

- **Short preparation time.**
  In quantum computation, we can't measure the final state of mixed state with one measurement. For example, if the state is

  $$|\psi\rangle = \alpha\,|0\rangle + \beta\,|1\rangle$$

  A single measurement will give with a probability of $|\alpha|^2$ for $|0\rangle$ and with probability $|\beta|^2$ for $|1\rangle$. As described in Ref. [13], We need about 350 experiments for each experimental value, distance between the traps, the interaction, the gate time, etc. In cold atoms system each cooling stage takes a certain time, for example:

  - 3D MOT loading - 20-50 sec
  - D1 cooling - 10 msec
  - Magnetic evaporation - 20-30 sec
  - optical evaporation - 3-5 sec

  In our second apparatus (that described in 123), the preparation time is approximately 70 sec. The total sequence duration that we get in this system for 20 parameters is

  $$350 \cdot 20 \cdot 70 \approx 6\ \text{day}$$

  We cannot ensure such a long time stability of our system due to fluctuation in the magnetic field, laboratory temperature, lasers stability, etc. In order to make the measurement is a feasible time (less than 1 day), we need approximately 8 sec per measurement.

- **A good separation between the atoms source chamber and the science chamber.**
  The atoms are released continually from a dispenser at a temperature of 300K and travel in all the vacuum chamber. To be able to detect single atom we need to avoid of traveling atoms in the science area. These atoms shorter the lifetime in the optical trap, and we can not reduce their temperature low enough. In the first group apparatus, we used a three-chamber configuration. In the middle chamber ("cooling chamber") we perform all the cooling process include magnetic evaporation that for magnetic evaporation apparently, this system is not needed. Therefore, we need one chamber for releasing the atoms and another chamber to manipulate them.

- **High NA in one axis.**
The requirement to create a high NA at least on one axis is made for a number of reasons. First, in order to load a single atom to microtraps, we need to create an optical trap with ω_0 smaller than 1.8 μm. Second, for the detection, we have a small number of photons, and we want to collect as much it possible. Previous work obtains an apparatus with NA=0.86 with an objective with NA=0.6 and a hemisphere lens on the optical viewport [21]. The working distance in those work is $\sim 150 \mu m$ from the window, and therefore all the beam need to be with total reflected angle to this surface. In a new work with cesium used with an objective with NA=0.92 but it was placed within the vacuum chamber [29]. Both techniques reach a high NA but insert a main constraint to the system - a part we want to avoid. In (4.2), I will describe a new method to use an objective with NA=0.65 which meets our requirements.

- **Avoid reflection photons scattering**.
In the first group apparatus, we have a science chamber with a small optical window (but with high NA from 3 axes) and 5% reflection per surface. We suspect that overheating during baking caused the Anti-Reflection coating (AR) to be damaged. As a result, the scattering photons from the windows surface created a large background in the detection area. To avoid it, we take one axis with high NA and all the other windows are taken far from the position of the atoms. In addition, we will bake the vacuum system up to 250C to avoid any damage to the AR coating.

- **Ability to perform high magnetic field.**
One of the main constraints in our system is the ability to control with high stability the interaction between two spin states. This is done by applying a magnetic field in the position of the atoms. As shown in (1.1), the magnetic field that we need for our system is ~202.2+-7 Gauss (non-interaction is at 209G). Therefore, we need two coils with Helmholtz configuration and with the chamber geometry decide the coils parameters (radius, distance from the atoms, number of threads). We already perform a high stability current control (40 ppm) in our group. The

Taking all these requirements with our experience we design a new system constrain two chambers, one as a source and second for cooling and experimental place (9). Our apparatus is one long glass chamber ("2D chamber") that connected to a hexagon chamber ("science chamber"). All the system will bake in order to create an ultra-high vacuum ($\sim 10^{-11}$ torr). In addition, the science chamber will be coated by Non-Evaporable Getter (NEG) coating which can improve the vacuum. In the 2D chamber, ^{40}K atoms are released from homemade dispenser with a temperature of 3..K. Then, the atoms are trapped by a 2D MOT that creates a string of cold atoms. A laser beam in the third axis pushes the atoms through a nuzzle to the science chamber. The atoms are collected and cooled in the second chamber by a 3D MOT. The 3D MOT consists of three counter-propagating circularly polarized beams with a retro-reflection configuration containing both cooling and repumping frequencies. The laser light at a wavelength of 767.7 nm for the

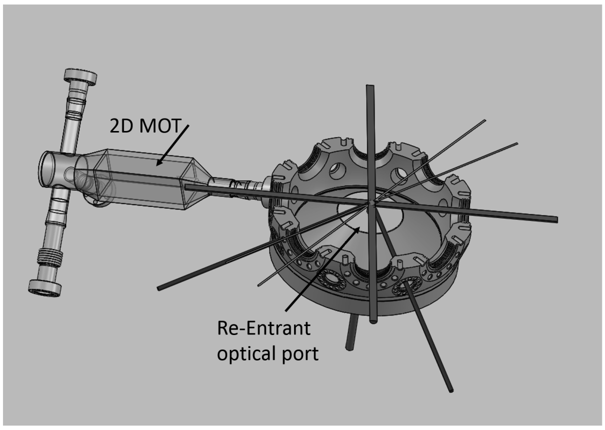

Figure 9: New apparatus 3D model. The atoms are released and capture in a 2D MOT. In the science chamber, we will apply a 3D MOT and D1 cooling from a 3 retro-reflection beams (red line). In addition, will induce a optical trap from 2 far of resunannce laser with 6° between them (green line). The detection beams will be with 68° from z axis (blue line). This angle is impotent to RSC detection. In our new apparatus, we get a working distance between the atom position and the last view port surface ∼12.5mm.

cooling and repump is generated from two DBR lasers with tapered amplifiers. Both lasers are offset-locked relative to a common master laser which is stabilized using saturated absorption spectroscopy in a vapor cell containing ^{39}K. The temperature in 3D MOT is limited due to the Doppler limit

$$T_D = \frac{\hbar\Gamma}{2k_B}$$

where k_B is the Boltzmann's constant, $\hbar$ is the reduced Plank's constant, and Γ is the natural line-width [17]. In ^{40}K, the Doppler limit is $T_D = 145\ \mu$K. Then we create a Gray Molasses cooling on the D1 transition to lower the atom temperature to $\sim 15\ \mu K$. For the D1 cooling, we used another DBR laser with a tapered amplifier. The laser is locked on the D1 transition of the ^{39}K using saturated absorption spectroscopy (separated system from the D2 transition locking system). The frequency is shifted (˜705 MHz) to the cooling D1 transition in ^{40}K by using AOMs. For the repump, we used the cooling beam and added a sideband by using home-made high-frequency Electro-Optic-Modulator. Both, cooling and repump, are phase locked that is necessary for D1 cooling. Next, we will load the atoms into an optical trap which will be created by 2 lasers of 50 W at 1064 nm wavelength. This laser needs to be orthogonal with linear polarization. The laser will focus to $\omega_0 = 250\ \mu$m and intersect at an angle of $\sim 14°$ at the center of the 3D MOT, creating a optical trap with $\sim 100\ \mu$K depth. Next, we will make evaporation by lowering the optical depth (namely laser power) up to T/T_F 0.5. Then we will open the optical microtrap beam and load atoms to it (more detail in (4.2))). Finally, we will reduce the microtrap power and open a gradient coil to spill the atom one by one up to a single atom remain.

4.2 Microtrap

As shown in , we already create in the first system a microtrap by using a homemade objective with NA=0.3. In the initial numerical calculations of the $\sqrt{\text{SWAP}}$ gate, we see that the NA have to be large (>0.8) in order to get a short time scale for the gate. This demand is a result of the aspect ratio between the radial and the axial frequencies in a Gaussian beam. To apply this demand we need to design objective with Hemisphere lens on the vacuum chamber (with very short working distance) or to design it to be in the vacuum chamber. To avoid building a system that is harmonized only to that without versatility, we offer a new scheme to overcome this problem with NA˜0.65. Optical trap frequencies are depended on the waist ω_0 in the radial axis and the Raleigh range z_R in the longitudinal axis.

$$\nu_r \propto \frac{1}{\omega_0}, \qquad \nu_z \propto \frac{1}{z_R}$$

For given NA the aspect ratio is given by $NA = \omega_0/z_R = \sqrt{2}\nu_z/\nu_r$ as shown in figure 111 the aspect ratio can be less then 1.6 with NA>0.85. To overcome this experimentally difficulty We propose to add a standing wave in the longitudinal axis. We can match the standing wave to the microtrap radial frequency and by this to get aspect ratio of ~ 1.1 (which equivalent to NA=1.28). The standing wave will be created from two laser beam 90° from the microtrap longitudinal axis and separated by $\sim 6°$. This will create a 2D "pancakes" with a distance of $\sim 10\ \mu$m between them (10).

4.3 Single Atom detection

The major open question is how to detect a single atom with spatial and the spin state resolved. In the last few years, there is a new technique of single atoms detection. Each one of them has advantages and disadvantages that will explain in this section.

- Fluorescence detection.
  The fluorescence imaging can't work in potassium 40 in optical lattice but may work for separated micro traps. It was shown, In litium6, that a fluorescence imaging of a single atom can work but the spatial width of the signal is $\sim 5\mu$m [3]. For fluorescence imaging, when We illuminate the atomic sample from the side with two counter propagating, horizontally polarized laser beams. We can capture the fluorescence photons with a high-resolution objective in the orthogonal axis (the same objective that creates the microtrap). By inducing a magnetic field, the spin states are resolved. For example, for 204 G the different between $|-9/2,-9/2\rangle_{^2S_{1/2}} \rightarrow |11/2,-11/2\rangle_{^2P_{3/2}}$ and $|-9/2,-7/2\rangle_{^2S_{1/2}} \rightarrow |11/2,-9/2\rangle_{^2P_{3/2}}$ is Γ. The photon per atom is ~ 60 photon/μs. To detect such low photon numbers down to a single photon resolution, we need a camera with a high quantum efficiency to detect as many photons as possible. Furthermore it is necessary that one photon creates a signal above the noise level. For these reasons we can use a EMCCD (Electron Multiplying Charge-Coupled Device).

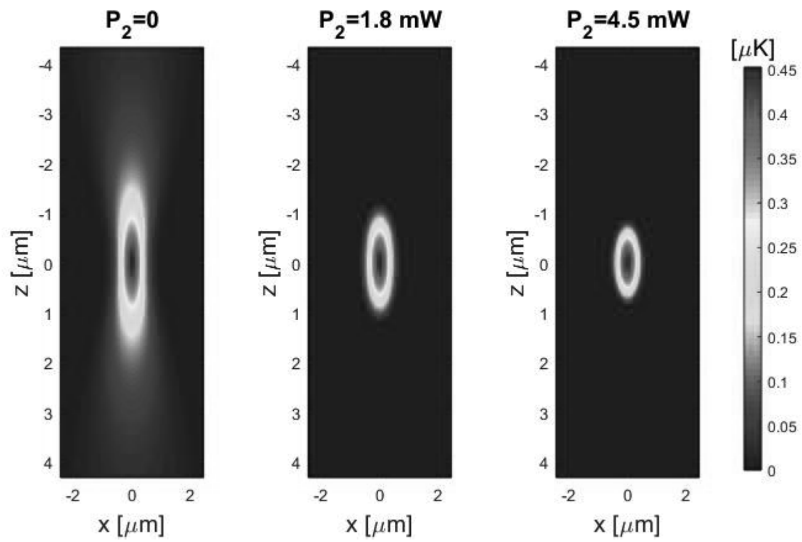

Figure 10: Microtrap potential Vs. the second beam power. In the left figure, We calculate the potential depth as without a second (standing wave) beam of a signal Gaussian beam with NA=0.65 and power of 2 μW. We open the standing wave beams and short increase the aspect ratio between the Rayleigh range and ω_0.

- Ranam SideBand Detection.

  Raman sideband cooling was first propose by Wineland et al. in 1995 and it done by using lasers and magnetic field [19]. By adding a magnetic field the relative energy between vibrational state of two Zeeman sub-level are split such that the state $|F, m_f\rangle_n$ and $|F-1, m_f+1\rangle_{n-1}$ are degenernte (F is the total spin number, m_f is the Zeeman index, and n is the vibrational state index). Then by using a Raman transition we can pump the atom from $|F, m_f\rangle_n \longrightarrow |F-1, m_f+1\rangle_{n-1}$. The cooling cycle is completed by optically pumping the atom back to the initial state. In order to be sure that the atom pump back to the initial state without changing its vibrational index, we need to work in the Lamb-Dicke regime [7]. Only recently it was performed also with ^{40}K [4].

  By cooling with Raman sideband technique, we can detect the number of atoms at each site due to their fluorescence without heating. The fluorescence rate for single atom is $\sim 60-80$ photom/sec and we can measure them with the EMCCD camera. The disadvantage of this technique is its incapability to distinguish between the atoms spin states and the complexity of its experimental system (lasers in D1 and D2 transition that include four different frequencies).

- 3D-MOT Detection.

  Another way to detect a single atom with high fidelity is to use 3D MOT. Although this is the initial phase of cooling and heats the atoms to a temperature of T_D it is an easy way to produce alot of photons per atom. The key advantage over other detection schemes is that the observation time and therefore the number of collected photons can be made almost arbitrarily large. Ultimately, it is only limited by the lifetime of the MOT, which is mainly determined by collisions with the background atoms.

4.4 Stern-Gerlach polarizing splitter

In an atomic interferometer, We can use a "beam splitter" that split and recombine two paths. For example, In an optical system, we can use a Polarized Beam Splitter control the light path depending on their polarization. In our system, we can switch, adiabatically, a single well to a double well by turning on a second optical trap next to the first one. A known example of this is the Stern-Gerlach experiment. This method is based on non-trapping atoms. We propose a new method, that similar to Stern-Gerlach but, for a trapped single atom beam splitter.

We start with a single atom in the ground state and a single micro trap at $x = 0$. The state of the atom is $|\psi(t=0)\rangle = \alpha|\downarrow\rangle_0 + \beta|\uparrow\rangle_0$. Then a second microtrap is, adiabatically, switched on at $x = d$. At the same time, a magnetic field, with a gradient $\frac{\partial B_z(x)}{\partial x}$, is implemented. The magnetic force at each state is a difference depending on their magnetic moment. Therefore, the state will start to oscillate with different frequencies. After a finite duration T, the states will evolve to $|\psi(t=T)\rangle = \alpha|\downarrow\rangle_0 + \beta|\uparrow\rangle_1$.

We can use this scheme to create a detection with spin depended. By adding to each qubit a new microtrap to the detection we translate the spin state to a spatial position.

4.5 $\sqrt{\text{SWAP}}$ Gate

My main goal in my Ph.D. is to apply a two-qubit gate in ultracold atoms apparatus. To do it we need to achieve the following goals.

- Build the system and load with high fidelity a single qubit with the same initial conditions.
- Developing a single atom spin-resolved detection.
- Control the parameters of the two-qubit gate: the interaction parameter and continuously change the distance between the qubits.

The two first goals s explained in the previous two sections. The control on the interaction parameter can be modified by Feshbach resonance. As shown in (1.1.1), the ^{40}K for our states Feshbach resonance is at 202.16G. To induce such magnetic field we can use the gradient coil with a Helmholtz configuration and increase the current to ~110 A. The last parameter is the tunneling energy, which proportional to the distance between the microtraps. As explained in (2.5), the two microtraps will induce from a single beam that will be divided at different angles (that translate to position) to several microtraps by AOD. Changing the rf frequencies different in the AOD will be translated into a different distance between them. One of the open questions is how to generate the microtrap trajectory in order to obtain a fast transfer to the gate and the same state at the end with high fidelity[18].

5 summery

In conclusion, this proposal suggests of creating a quantum computation system with cold atoms apparatus. First, We need to build the new apparatus with good conditions. There are still some open questions like:

- Can we get enough atoms at low temperature without other cooling states?
- In which detection method we need to work?

The second stage will apply a Stern-Gerlach measurement with our new scheme. Finally, to create a $\sqrt{\text{SWAP}}$ gate in our system and tune the parameters in order to get high fidelity.